Ablative thermo-protective properties of epoxy composites with high-melting metal nanooxides*)

Wojciech Kucharczyk[1] (ORCID ID: 0000-0002-7593-8592), **Mohamed Bakar**[2] (0000-0002-0302-0010), **Bohumír Strnadel**[3] (0000-0003-3401-5027), **Anita Białkowska**[4, **] (0000-0002-4868-5833), **Wojciech Żurowski**[1] (0000-0001-6368-1489), **Robert Gumiński**[1] (0000-0001-9868-6992)

DOI: https://doi.org/10.14314/polimery.2025.2.2

Abstract: The influence of the hardener (polyaminoamide) and nanofillers (mixture of TiO_2 and Al_2O_3 nanooxides) on the thermal protective ablative properties of epoxy resin (Epidian 52) was investigated. The composites were exposed to exhaust gases at temperatures above 1900°C for 120 s. A statistical analysis of the results obtained was performed. The best thermo-protective ablative properties showed the composite based on resin cured with the hardener (mass ratio of epoxy/hardener = 1:1) and 5 vol% of nanoparticles mixture containing 80% Al_2O_3 and 20% TiO_2.

Keywords: ablative properties, thermo-protective properties, epoxy composites, high-melting metal nanooxides.

Ablacyjne termoochronne właściwości kompozytów epoksydowych z wysokotopliwymi nanotlenkami metali

Streszczenie: Zbadano wpływ utwardzacza (poliaminoamid) i nanonapełniaczy (mieszanina nanotlenków TiO_2 i Al_2O_3) na ablacyjne termoochronne właściwości żywicy epoksydowej (Epidian 52). Kompozyty poddano działaniu gazów spalinowych o temperaturze powyżej 1900°C przez 120 s. Przeprowadzono analizę statystyczną uzyskanych wyników. Najlepsze właściwości miał kompozyt na bazie żywicy utwardzanej taką samą ilością utwardzacza (żywica/utwardzacz 1:1) z dodatkiem 5% obj. mieszaniny nanocząstek Al_2O_3 (80%) i TiO_2 (20%).

Słowa kluczowe: właściwości ablacyjne, właściwości termoochronne, kompozyty epoksydowe, wysokotopliwe nanotlenki metali.

The impact of high-temperature heat sources on building load-bearing structures, machines, devices and directly on people has created the need to design composite materials for thermal protective coatings and thermal shields. The experimental work conducted is aimed at acquiring knowledge about the main phenomena occurring in the ablation of nanocomposites, in the context of thermal protective features of these materials used in fire situations.

The ablation phenomenon is a heat and mass exchange process, during which physical changes, chemical reactions and irreversible structural changes in the material occur, as well as heat absorption. The ablation process is initiated and maintained by external energy sources [1–3]. Ablation of the material begins when the temperature on the surface exposed to the heat source reaches the temperature of thermal decomposition of the material. The ablation temperature for organic materials is in the range of 150–300°C. In the ablation zone two areas are distinguished [1–4]: primary decomposition area – the material decomposition processes are initiated at the ablation temperature, and secondary reaction zone at a temperature higher than the ablation temperature – new chemical compounds are formed from the products of thermal decomposition of the matrix and fillers.

Ablative materials are used in the arms industry [4–7], space technology [6–9], in the design of protective materials for load-bearing structures of buildings [10, 11], in rail transport and construction of underground tunnels [12, 13] and wherever heat fluxes may pose a threat to people [14, 15]. Ablative materials are also used for covers of on-board tape recorders [16].

[1] Faculty of Mechanical Engineering, Casimir Pulaski Radom University, 29 ul. Malczewskiego, 26-600 Radom, Poland.

[2] Independent Researcher, Poland.

[3] VŠB-Technical University of Ostrava, 17. listopadu 15, 708 00, Ostrava-Poruba, Czech Republic.

[4] Faculty of Applied Chemistry, Casimir Pulaski Radom University, ul. Malczewskiego 29, 26-600 Radom, Poland.

*) Material contained in this article was presented at the XXI Scientific-Technical Conference on "Polimery i Kompozyty Konstrukcyjne" (KOMPOZYTY 2024), 22–25 October 2024, Wisła, Poland.

**) Author for correspondence: a.bialkowska@urad.edu.pl

Composites with good protective properties in terms of thermal shock and fire buffering are sought. Composite polymer coatings with typical ablative composite matrices are known. Such matrices may be silicone resin [17], phenolic resin [18–22] or epoxy resin [15, 23–31] with fillers increasing the thermal stability of the composite [18–21, 23–28, 32]. Pure resins are good ablative materials. However, they require reinforcement [33], due to their low decomposition temperature, porosity, and fragility of the ablative layer [34]. Addition of powders [17, 18, 22, 24, 25, 35–37], nanopowder [17, 29, 38], fibres [19, 20, 23, 33, 39, 40] or reinforcing plates of high melting temperatures [17, 36, 41] build a composite structure that substantially improves thermoprotective [37, 38], thermomechanical [38, 41] and mechanical [32, 33, 42] properties of a polymer ablative composite.

Good thermal protective properties are provided by polymer shields with typical ablative composite matrices, such as silicone [17], phenolic [18–22] and epoxy [15, 23–31] resins modified with fillers increasing the thermal stability of the material [18–21, 23–28, 32]. Resins are the basic ablative materials, but they require reinforcement [33] due to their low decomposition temperatures and the porosity and instability of the ablative layer [34]. Modification with micropowders [17, 18, 22, 24, 25, 35–37], nanopowder [17, 29, 38], glass, carbon, aramid fibers [19, 20, 23, 33, 39, 40] or "honey comb" type spacers with a high melting point [17, 36, 41] makes it possible to constitute a material with good thermal protective [37, 38], thermomechanical [38, 41] and mechanical [32, 33, 42] properties.

Despite many studies, the quantitative and qualitative relationships between the components and the thermal protective properties of ablation materials remain unexplored [43].

The aim of this study is to understand the basic phenomena occurring in the ablation processes of epoxy resin-based nanocomposites in the context of their thermal protective properties of materials. The research conducted provides an opportunity to develop ablative composites that protect people, machines, devices, and structures from exposure to heat flow. The aim of this work was to investigate the effect of the type of metal nanooxides on the ablation properties of epoxy resin-based nanocomposites, i.e., the temperature of the back surface of the sample and the ablation mass loss.

EXPERIMENTAL PART

Materials

The liquid epoxy resin Epidian 52 produced by Ciech Sarzyna Co. (Nowa Sarzyna, Poland) was selected as the matrix for the tested nanocomposites. The factors determining this choice were: physicochemical properties, ease of processing, low price, and availability on the market. Epidian 52 is a mixture of a low molecular weight resin and an active diluent. It reacts with various hardeners (Table 1). Polyaminoamide (trade name PAC) produced by Ciech Sarzyna Co. (Nowa Sarzyna, Poland) was selected as the hardener [44]. The selected PAC is used to modify and harden low molecular weight epoxy resin. It is a viscous liquid with low reactivity. In addition, it hardens epoxy resins in a wide range of weight ratios of resin and PAC. Due to the need to carry out various technological operations, the stability of the epoxy composition with the PAC hardener is important. This takes several hours, and the resin is completely hardened in 4–7 days at room temperature [44]. Two kinds of high-melting metal nanooxides [28] (both produced by Sigma-Aldrich Co, USA) – titanium dioxide TiO_2 (as powder) and aluminum trioxide Al_2O_3 (as nanofibers) were chosen to modify the epoxy resin [45].

Statistical analysis

Statistical analysis was performed according to developed standards [46].

The number of tested composites (Table 1), equal to the number of scheduled experiments (N = 8), was determined based on the experiment plan described by an orthogonal 1st order full-factorial matrix of type $2^3 = 8$. It included single replications, where two state levels (lower level "–1" and upper level "+1") and three independent input variables (x_i, where i = 1, 2, 3) [46]:

x_1 – volumetric content of nanofillers mixture in composite:

lower level "–1" means 2 vol%

T a b l e 1. The tested samples composition

	Samples									
	1	2	3	4	5	6	7	8	9	10
Both nanofillers, vol%	2	2	5	5	2	2	5	5	none	none
PAC, phr	60	60	60	60	100	100	100	100	60	100
Al_2O_3, mix%	20	80	20	80	20	80	20	80	none	none
TiO_2, mix%	80	20	80	20	80	20	80	20	none	none
x_1	-1	-1	+1	+1	-1	-1	+1	+1		
x_2	-1	+1	-1	+1	-1	+1	-1	+1		
x_3	-1	-1	-1	-1	+1	+1	+1	+1		

upper level "+1" means 5 vol%

x_2 – weight fraction of Al_2O_3 to the sum of the weight of both nanofillers (Al_2O_3 + TiO_2):

lower level "–1" means 20% Al_2O_3/80% TiO_2

upper level "+1" means 80% Al_2O_3/20% TiO_2

x_3 – weight proportion of PAC hardener relative to Epidian 52 resin:

lower level "–1" means Epidian 52 + 60 phr of PAC

upper level "+1" means Epidian 52 + 100 phr of PAC

(phr – means weight proportion of hardener parts per 100 parts of resin).

The components of the response variable "y" (the output parameters) [46] are the average:

– maximum temperature of rear sample wall surface $T_{s\_max}(x_i)$, °C

– relative ablative (erosive) weight loss $U_a(x_i)$, % after 120 s of treatment with hot combustion gases.

The regression and interaction coefficients (b_i) of all function components have been calculated. The threshold relevance of the regression coefficients (b_i) and estimation of their effect on the output parameters (y) were determined. The output value was calculated from Equation 1 [46]:

$$y = (b_0 + b_1x_1 + b_2x_2 + b_3x_3 + b_{12}x_1x_2 + b_{13}x_1x_3 + b_{23}x_2x_3 + b_{123}x_1x_2x_3) \pm s(y) \quad (1)$$

Additionally, the variance $s(y)$, regression error $s(b_i)$ and interaction coefficients $s(b_i)$, as well as the level of their statistical significance (b^3_{sign} b_i) have been determined based on t-Student test at the confidence level $a_p = 0.05$ [46].

Samples preparation

All composites for ablation tests were obtained in laboratory conditions. Samples 1–8 (Table 1) was prepared according to the following procedure:

– weighed amount of nanofillers mixture (2 or 5 vol% of total content in composites) was added to epoxy matrix and the components were mixed by using a Hielscher UP200H (Teltow, Germany) homogenizer (amplitude – 48%, frequency – 100% and power 40 W) for 5 min

– the obtained mixture was cooled to room temperature,

– mixing with hardener PAC (60 phr or 100 phr),

– mechanical homogenization of the obtained composition for 5 min,

– pouring the mixture into previously prepared silicon forms,

– curing of epoxy compositions in the molds during 4 days at room temperature and then post-cured at 70°C for 12 h.

The reference samples 9 and 10 (unmodified, only cured epoxy resin) were obtained by adding the hardener to the epoxy resin (Table 1) and mixing both components (also for 5 min). Sample 9 contained 60 phr of PAC, while sample 10 contained 100 phr of this hardener (Table 1).

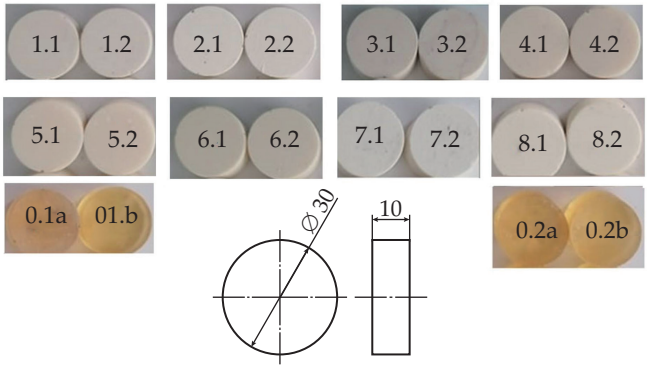

Fig. 1. View of the samples and their dimensions

A total of 20 samples (16 composites and 4 pure cured resin samples) with dimensions of 30 × 10 mm (diameter × thickness) were prepared for the tests (Fig. 1).

Methods of ablative properties evaluation

All composite samples were weighed and then mounted on plasterboard shields on a stand with an ablation gun designed for ablation tests [23, 26, 28, 29, 38]. The ablation test lasted 120 s. The examined composites were exposed to a stabilized hot stream of combustible gases. The heat came from burning a propane-butane mixture (containing 65% propane and 35% butane). The temperature of flammable gases was above 1900°C.

The flame stabilized with an ablation gun, whose axis was set perpendicularly to the front surface of the sample and the gun nozzle was placed 30 mm away from the surface of the ablation surface.

The stand designed in this way allows stand to stabilize the flame, unify the temperature on the ablation surface as well as ensure the repeatability of results for all test samples. Before testing, the gun was preheated to stabilize and equalize its temperature. The uniform, pale yellow, becoming almost white, indicates stabilization of the flame and uniform heating of the sample surface. The entire sample surface was within the range of the heat flux with the temperature of flammable gases above 1900°C.

The following temperatures were recorded during the experiment:

– the ablative surface T_{pa} with a thermovision camera Thermo Tracer NEC H2640 (Yokohama, Japan) at the 60th second of each test;

– the ablative surface $T_{pa}(T)$ using an optical pyrometer OPTCT2MHCF by Optris GmbH (Berlin, Germany), set at an emissivity of ε = 0.95 and featuring a continuous electronic recording of temperature variations using Compact Connect 1.7.3 software;

– the rear sample wall surface $T_s(T)$ by means of TP-204N (NiCrSi-NiSi) thermocouple by Czaki Thermo-Product using a measurement module USB-4718 by Advantech (Taiwan).

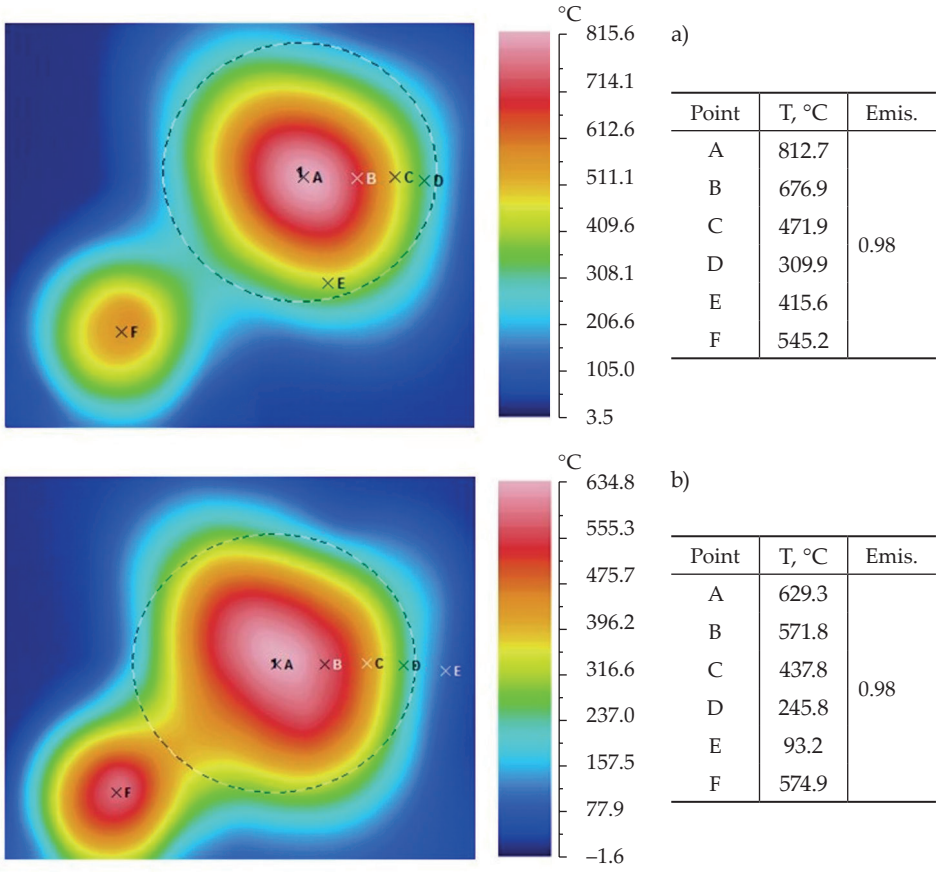

a)

Point	T, °C	Emis.
A	812.7	0.98
B	676.9	
C	471.9	
D	309.9	
E	415.6	
F	545.2	

b)

Point	T, °C	Emis.
A	629.3	0.98
B	571.8	
C	437.8	
D	245.8	
E	93.2	
F	574.9	

Fig. 2. Temperature fields on the ablative surface after 60 s of heat flux exposure: a) sample 1, b) sample 10

RESULTS AND DISCUSSION

The temperature distribution on the ablation surfaces of the analyzed samples was recorded using a thermal imaging camera. Figure 2a shows the results of the temperature measurement on the surface of sample 1 (2 vol.% of the nanoparticle mixture containing 80% TiO_2 and 20% Al_2O_3, resin cured with a smaller amount of hardener) in the 60th s of the ablation test. The brightest, almost white area in the center of the sample (point A) corresponds to the highest surface temperature (812.7°C). However, the red areas (point B) correspond to their lower value (678.9°C). Lower temperatures are further from the hot spot of the sample. The orange-yellow point C, yellow point E and green point D in the upper part of the sample are caused by the rising of the hot gas stream upwards. However, in the case of pure cured epoxy resin, the maximum temperature at the ablation surface is more than 180°C lower (629.3°C) as illustrated in Fig. 2b, which proves the faster heat transfer at the gas-solid (sample material) interface.

The ablative surface temperature T_{pa} was assumed as an indirect input testing parameter (Fig. 8). Additionally, it was assumed as the first type boundary condition for Dirichlet (determined by the temperature distribution anytime on the surface of the body), enabling the resolution of Fourier-Kirchhoff differential equation of unsteady heat conduction in solids. Epoxy composites achieve a higher temperature on ablative surfaces than unmodified, pure epoxy resin (Fig. 3), which proves their slower conduction of heat flux.

The mentioned temperature of the ablative surface relates to the heat transfer at boundary between gas and solid-state material, the heat conduction through the wall of the composite and the ablative processes taking place on the surface layer (endothermic chemical reactions, polymer degradation and different structural changes). The value of this temperature depends on the physical properties of solid material and gas, as well as insulating wall geometry (Fig. 4).

Reference samples (9 and 10) have an average temperature on ablation surfaces lower by about 200–250°C T_{pa} (Fig. 4). Therefore, they have higher thermal diffusivity values, i.e., they show a greater ability to equalize temperature across the wall thickness. These are unfavorable thermal protective properties of pure, cured epoxy resins.

The temperatures T_{s_max} determined during these tests indicate the possibility of using the material as a protective cover.

In the tests performed, the surface temperature of the rear walls of the sample $T_s(T)$ was measured for 120 s, and their distributions for all composites and pure resins are shown in Fig. 5.

Epoxy resin-based nanocomposites 3 and 4 modified with 5 vol% of nanoparticle mixture and resin cured by less addition of hardener (60 phr of PAC), had the lowest average temperatures T_{s_max} = 58°C from all tested

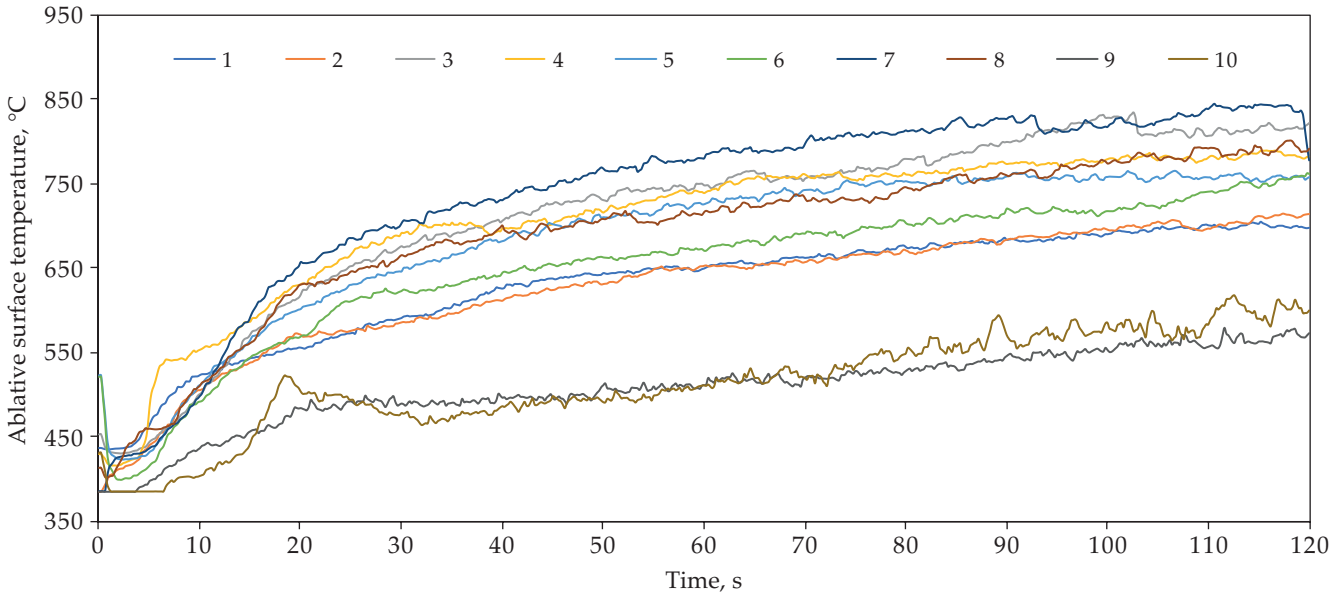

Fig. 3. Influence of sample exposure time with heat flow on the surface ablation temperature

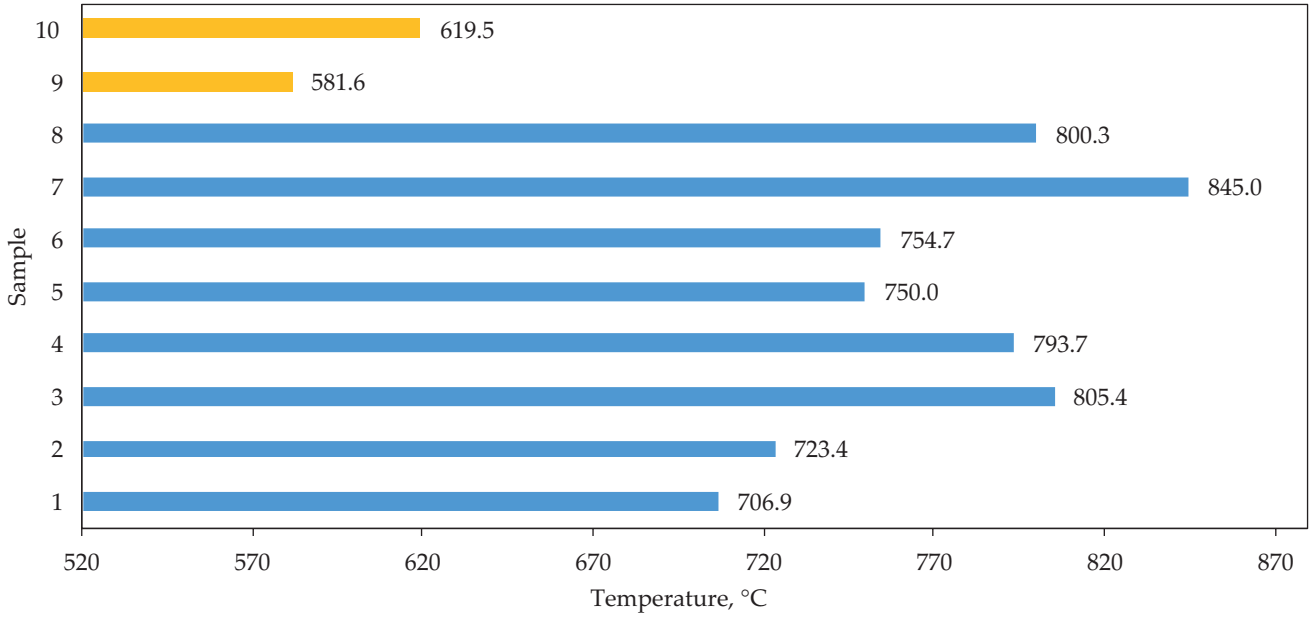

Fig. 4. Average maximum temperature on the ablation surface T_{pa_max} for the tested composites after 120 s of heat flow exposure

samples (Fig. 6). The reference samples reached the highest temperature on the rear sample wall surfaces, T_{s_max} = 66°C. This proves their worse thermal protection properties.

The heat flux density passing through a flat wall is determined by Pécelt's law (2), which shows that under steady-state conditions (q = const), the temperature of the medium behind the wall will have a value determined by Equation 2.

$$q = \frac{T_{p1} - T_{p2}}{r_{kp}} \quad (2)$$

where: q – heat flux density (W/m²); T_{p1} – temperature of the medium in front of the face of the wall (°C); T_{p2} – temperature of the medium behind the back wall (°C).

So far, no known engineering materials (metals, ceramics, polymers, composites) have shown a specific resistance to heat transfer r_{kp} of such a high value as to constitute a long-term thermal shield reducing the temperature in the range up to $\Delta T = T_{p1} - T_{p2} \cong 2000$°C. This is feasible with insulating walls with a thickness of several meters, which eliminates the possibility of using this method of thermal insulation, e.g., in transport [4, 23].

For composites:
4: $\Delta T = T_{p1} - T_{p2}$ = (794 – 58)°C = 736°C.
3: $\Delta T = T_{p1} - T_{p2}$ = (805 – 58)°C = 747°C.

For pure, cured epoxy samples:
Sample 9: $\Delta T = T_{p1} - T_{p2}$ = (582 – 66)°C = 516°C
Sample10: $\Delta T = T_{p1} - T_{p2}$ = (620 – 66)°C = 554°C

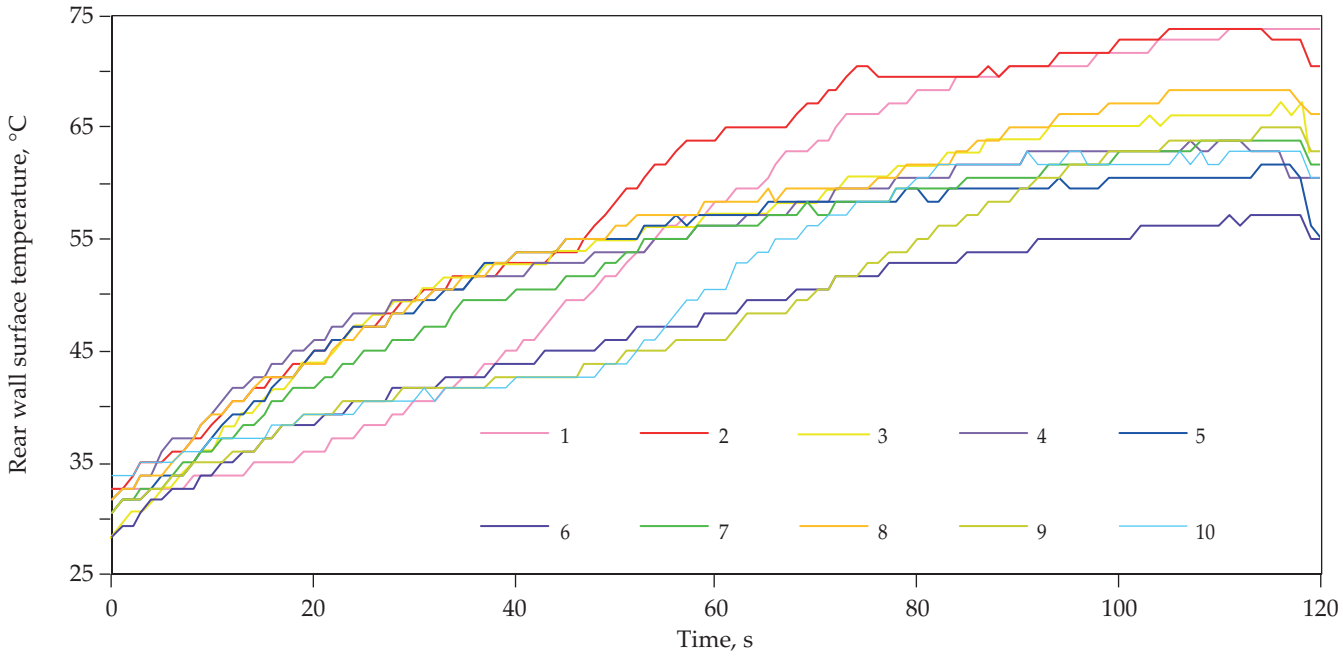

Fig. 5. Influence of sample exposure time with heat flow on the rear sample wall surface temperature

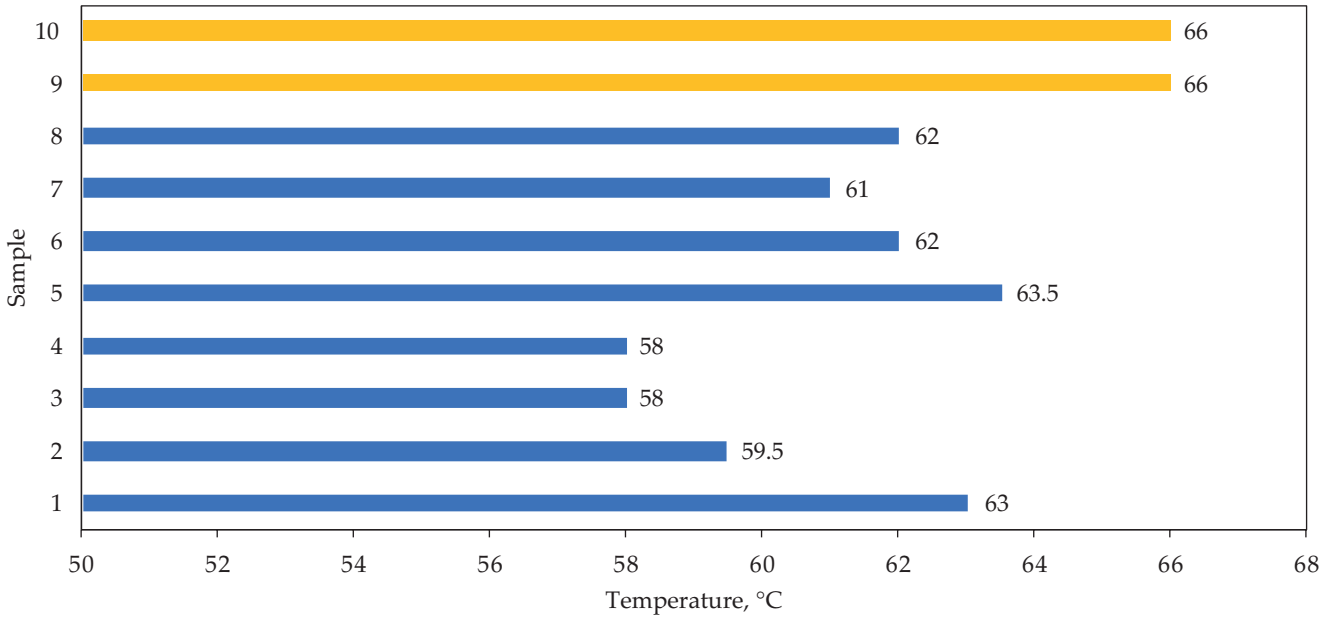

Fig. 6. Average maximum temperatures (T_{s_max}) on the surface of the back wall of the tested compositions after 120 s of heat exposure

It follows from the above that under steady-state conditions, according to Pécelt's law, the specific resistance to heat transfer r_{kp} for epoxy nanocomposites is almost 40% higher compared to cured pure epoxy resin.

The composites are characterized by high temperature on the ablation surface T_{pa} and low temperature on the surface of the back wall of the sample. The large gradient of the mentioned temperatures causes high thermomechanical stresses in the material, which may often lead to the destruction of the ablation shield [23].

Therefore, the loss of composite mass due to erosive ablation (U_a) seems to be important during this evaluation. The smaller the mass loss of the ablation layer, the greater the thermal stability of the composite. As a result of erosion of thermally stable composites, a thicker top working layer [23] remains, which is advantageously characterized by a low thermal conductivity coefficient $l(T)$.

As can be seen, sample 8 showed the smallest (21%) weight loss, thus showing the smallest erosive wear after 120 s of heat exposure. Composites 4 and 7 showed a slightly more weight loss, indicating worse thermal protection properties (Fig. 7 and Table 2). It should be noted that thermal exposure of reference samples (pure epoxy resin) resulted in up to three times greater U_a mass loss compared to the obtained composites (57% and 62%).

The best thermal insulation properties are indicated as underlined bold, and the worst underlined in italic.

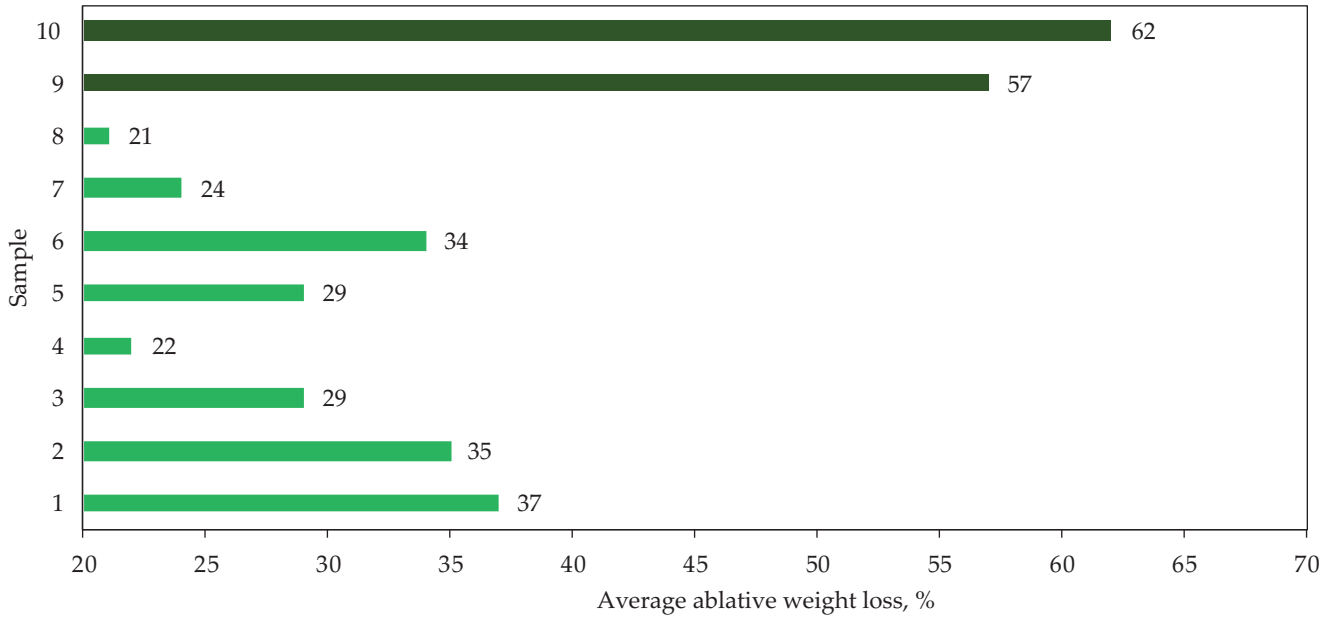

Fig. 7. Influence of 120 s of heat exposure on the weight loss (U_a) of the tested composites

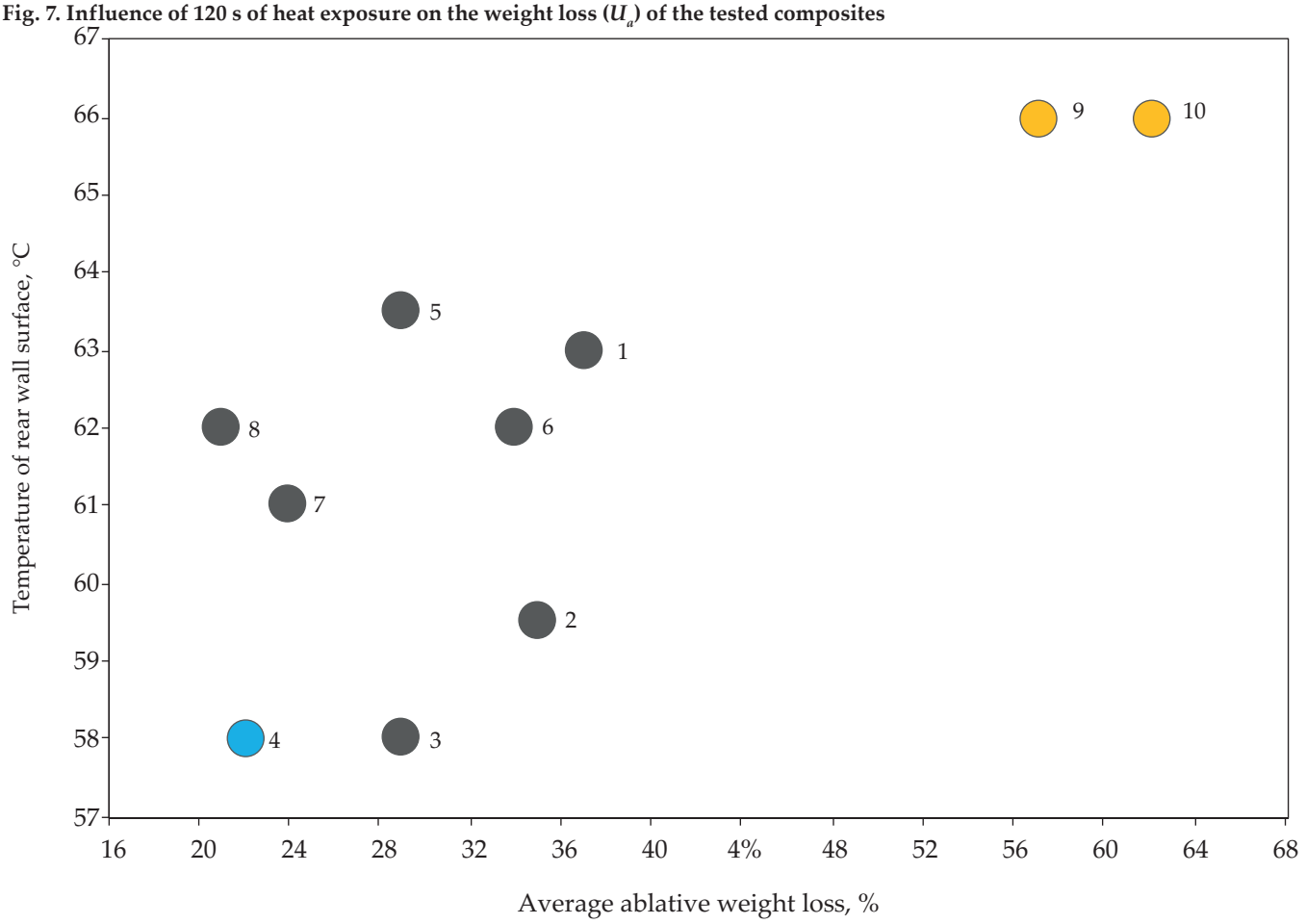

Fig. 8. Average weight loss (U_a) and maximum temperature on the rear sample wall surface (T_{s_max}) for phase compositions after 120s of the heat flow exposition

T a b l e 2. Ablation test results of samples exposed to heat for 120 s

	1	2	3	4	5	6	7	8	9	10
T_{pa_max}, °C	707	723	805	794	750	755	845	800	582	620
T_{s_max}, °C	63	59.5	**58**	**58**	63.5	62	61	62	*66*	*66*
U_a, (%)	37	35	29	**22**	29	34	24	**21**	*57*	*62*

T a b l e 3. Regression and interaction coefficients of experimental plane

Parameter	b_0	b_1	b_2	b_3	b_{12}	b_{13}	b_{23}	b_{123}	$s(y)$	$s(b_i)$	b_{sign}
T_{s_max}, °C	60.9	–1.13	–0.50	1.25	0.75	0.50	0.38	–0.13	1.61	0.57	1.31
U_a, %	28.8	–4.82	–0.80	–1.91	–1.54	0.19	1.44	–0.37	1.33	0.47	1.08

Table 2 summarizes the results of the ablation tests performed, i.e., maximum surface temperature ablation T_{pa}–max, maximum temperature of the rear surface of the ablation sample T_{s_max} and ablation mass loss U_a. The best thermal protection properties of tested samples are marked in bold and the worst – in italics.

As mentioned, the best thermos-protective properties have composites that were characterized by the lowest values of the maximum rear wall surface temperature T_{s_max}. As can be seen, composites 3 and 4 showed the greatest temperature reduction and the smallest loss of ablation mass (U_a). However, composites 8 and 4 showed the highest thermal stability and low thermal conductivity. After exposure to heat, they had the greatest thickness, most internally consistent-and were characterized by good adhesion to the working layer of the original ablative material and low conductivity.

Hence, the best thermoprotective properties had 4 (Fig. 8). The worst thermo-protective properties were shown by samples of pure, unmodified cured epoxy resin (№ 0.1 and № 0.2).

Statistical analysis of ablation results

The results of the ablation tests were used for statistical calculations of all input parameters of the function. Regression and interaction coefficients bi of both functions were calculated. The statistical analysis of the test results allowed us to determine the threshold significance of the regression coefficients bid and to estimate their impact on the output parameters "*y*". The output value of "*y*" was calculated from the following experiment objective equation (1) [46]. Moreover, the variance s(y), errors of the regression coefficients $s(b_i)$ and the level of their statistical significance (b^3_{sign} b_i) were determined based on the Student's t-test with a confidence level of $a_p = 0.05$ [46]. The calculated values are presented in Table 3. The parameter bi is marked in bold – it is smaller than bsign but is subject to the error $s(b_i)$, which, when considered when calculating b_i, allows us to estimate the sum of b_i and $s(b_i)$ as larger than b_{sign}, that is, still significant statistically [46].

Calculated regression and interaction coefficients – b_i and their level of significance (b^3_{sign} b_i), the following regression Equations 3 and 4 of the components of the response function "*y*" were formulated:

$$T_{s\_max}(x_i) = (60.9 - 1.13x_1 + 1.25x_3 - 0.75x_1x_2) \pm 1.61°C \quad (3)$$

$$U_a(x_i) = (28.8 - 4.82x_1 - 0.80x_2 - 1.91x_3 + - 1.54x_1x_2 + 1.44x_2x_3) \pm 1.33\% \quad (4)$$

The coefficients of response function $T_{s\_max}(x_i)$ equation (3) and $U_a(x_i)$ equation 4 indicate the following statements:

– The amount of PAC hardener used to cross-link the resin (b_3) has a significant effect on the temperature of the rear wall surface. The increase in the quantity of hardeners caused an increase in temperature which resulted from the positive value of the coefficient b_3.

– The effect comparable to x_3 has the code variable x_1, which means the volumetric fraction of nanofillers (Al_2O_3 + TiO_2). The higher the content of nanoparticles, the lower the temperature of the rear wall surface T_{s_max}.

– The combined variables x_1 and x_2 (b_{12}) have little influence on the value of the temperature T_{s_max}. The simultaneous increase in the content of used nanoparticles and the quantity of Al_2O_3 in the mixture (80% Al_2O_3 and 20% TiO_2) caused an increase in T_{s_max}.

– The erosive mass loss depends on the volume fraction of the mixture of nanofillers used (Al_2O_3 + TiO_2). A negative value of the coefficient b_1 indicates that the increase in the quantity of nanoparticles in the composite leads to a decrease in the erosive weight loss U_a.

– The variable x_2, denoting the content of Al_2O_3 nanofibers in relation to the sum of the masses of used nanofillers, has a small influence on the erosive weight loss.

– Code variable x_3 denoting the mass fraction of the hardener significantly influences the value of the ablative weight loss. The results indicate that increasing the amount of the hardener in the sample caused a decrease in U_a.

– Variables x_1 and x_2, in interaction, denoting respectively the share of Al_2O_3 in the mixture (Al_2O_3 + TiO_2) and the content of both nanofillers in the composite significantly affect the U_a value. Increasing these values leads to reduced erosive weight loss.

– The simultaneous increase in the content of Al_2O_3 in the nanofillers mixture and the hardener causes the increase of U_a, which results from the positive value of b_{23}.

CONCLUSIONS

Composites modified with nanofillers (Al_2O_3 nanofibers and TiO_2 nanopowder) showed much better heat protection and thermo-protective properties than virgin unmodified cured epoxy resin, i.e., lower T_{s_max} temperature, up to 40% higher specific resistance values to heat transfer r_{kp} and even three times lower ablative weight loss U_a. The best thermo-protective ablative properties had the composite based on resin cured with the hardener (mass ratio of epoxy resin/hardener = 1:1) and 5 vol% of nanoparticles mixture containing 80% Al_2O_3 and 20% TiO_2. This is associated with the lowest temperature of

the rear wall surface (T_{s_max} = 58°C) and the lowest erosive weight loss (U_a = 22%). The lowest ablative weight loss (U_a = 21%) was shown by the composite containing 5% nanofillers and a greater amount of Al_2O_3 nanofibers than TiO_2 powder (80% Al_2O_3 and 20% TiO_2 into mixture) and which was cured with the same amount (100 phr) of PAC hardener. This composite was characterized by the best thermal stability, cohesion of the ablative layer, therefore the best resistance to thermomechanical stresses and the ability to create a passive ablative layer. The nanocomposites based on Epidian 52 resin modified with 5 vol% of nanoparticle mixture (20% Al_2O_3+80% TiO_2 or 80% Al_2O_3+80% TiO_2) and cured by less amount of hardener (60 phr of PAC), attained the lowest average temperatures T_{s_max} = 58°C from all analyzed compositions. In the case of composites with the same amounts of nanofillers in the mixture, the increased amount of the hardener caused an increase in the temperature of the rear wall surface T_{s_max} and a decrease in ablative weight loss U_a.

Authors contribution

W.K. – conceptualisation, methodology, research; A.B. – validation, research, writing-review; M.B. and B.S. – writing and editing; R.G. – methodology and editing, W.Ż. – conceptualisation, supervision, visualisation.

Funding

The research was not funded.

Conflict of interest

The authors declare no conflict of interest.

REFERENCES

[1] Lin W.S.: *International Journal of Heat and Mass Transfer* **2005**, *48(25-26)*, 5504. https://doi.org/10.1016/j.ijheatmasstransfer.2005.06.040

[2] Feng-Er Yu. Study on the ablation materials of modified polyurethane/polysiloxane. Unpublished doctoral dissertation. Guangzhou: National Sun Yat-sen University, Materials Science and Engineering Department, **2004**.

[3] Dimitrenko Y.I.: *Composites Part A: Applied Science and Manufacturing* **1997**, *28(5)*, 453. http://doi.org/10.1016/S1359-835X(96)00144-3

[4] Młynarczyk K., Lon wic F., Podkościelna B. *et al*.: *Polimery* **2022**, *67(3)*, 102. https://doi.org/10.14314/polimery.2022.3.2

[5] Clemens H.P., Ward Y.C.: "Nozzle fabrication technology for large RDTTs", *YRT* **1966**, *9*, 48.

[6] Natali M., Kenny J.M., Torre L.: *Progress in Materials Science* **2016**, *84*, 192. https://doi.org/10.1016/j.pmatsci.2016.08.003

[7] Caporale A.M., Airoldi A, Natali M. *et. al*.: *Composites Part A:Applied Science and Manufacturing* **2022**, 159, 107035. https://doi.org/10.1016/j.compositesa.2022.107035

[8] http://www.nasa.gov/centers/ames/research/humaninspace/25th_shuttle.html

[9] Quagliano Amado J.C., Germán Ross P., Beck Sanches N. *et al*.: *Open Chemistry* **2020**, *18*, 1452. https://doi.org/10.1515/chem-2020-0182

[10] https://www.nist.gov/publications/collapse-world-trade-center-towers-final-report-federal-building-and-fire-safety

[11] https://www.ce.memphis.edu/3121/stuff/general/aibs_2002_wtc.pdf

[12] Haack A.: *Tunnelling and Underground Space Technology* **2004**, *19(4-5)*, 305. https://doi.org/10.1016/j.tust.2004.01.007

[13] Ono K, Otsuka T.: "Fire design requirement for various tunnel", Material from 32nd ITA – World Tunnel Congress, Seoul, South Korea, 25 April 2006.

[14] Pieniak D., Walczak A., Oszust M. *et al*.: *Materials* **2022**, *15(1)*, 57. https://doi.org/10.3390/ma15010057

[15] Wang X., Nabipour H., Yong-Chun K. *et al*.: *Progress in Organic Coatings* **2022**, *172*, 107095. https://doi.org/10.1016/j.porgcoat.2022.107095

[16] Paszkiewicz S., Pawelec I., Szymczyk A. *et al*.: *Polimery* **2021**, *61(3)*, 172. https://doi.org/10.14314/polimery.2016.172

[17] Yuan W., Wang J., Song H. *et. al*.: *Composite Structures* **2018**, *193*, 53. https://doi.org/10.1016/j.compstruct.2018.03.031

[18] Kucharczyk W., Przybyłek P., Opara T.: *Polish Journal of Chemical Technology* **2013**, *15(4)*, 49. https://doi.org/10.2478/pjct-2013-0067

[19] Pulci G., Tirillň J., Marra F. *et al*.: *Composites: Part A: Applied Science and Manufacturing* **2010**, *41(10)*, 1483. https://doi.org/10.1016/j.compositesa.2010.06.010

[20] Bahramian A.R.: *Iranian Polymer Journal* **2013**, *22*, 579. https://doi.org/10.1007/s13726-013-0157-z

[21] Zhou L., Sun X., Chen M. *et al*.: *Composite Structures* **2019**, *215*, 278. https://doi.org/10.1016/j.compstruct.2019.02.053

[22] Kuppusamy R., Swati N., Santoshi M. *et al*.: *Advances in Materials Science and Engineering* **2022**, *2022*, 7808587. https://doi.org/10.1155/2022/7808587

[23] Kucharczyk W.: *Przemysł Chemiczny* **2010**, *89(12)*, 1673.

[24] Bakar M., Kucharczyk W., Stawarz S.: *Polymers and Polymer Composites* **2016**, *24(8)*, 617. https://doi.org/10.1177/096739111602400808
[25] Camino G., Tartaglione G., Frache A. *et al.*: *Polymer Degradation and Stability* **2005**, *90(2)*, 354. https://doi.org/10.1016/j.polymdegradstab.2005.02.022
[26] Kucharczyk W., Dusiński D., Żurowski W. *et al.*: *Composite Structures* **2018**, *183*, 654. https://doi.org/10.1016/j.compstruct.2017.08.047
[27] Krzyżak A., Kucharczyk W., Gąska J. *et al.*: *Composite Structures* **2018**, *202*, 978. https://doi.org/10.1016/j.compstruct.2018.05.018
[28] Stawarz S., Witek N., Kucharczyk W. *et al.*: *International Journal of Mechanics and Materials in Design* **2019,** *15(3)*, 585. https://doi.org/10.1007/s10999-018-9432-7
[29] Kucharczyk W., Bakar M., Żurowski W. *et al.*: *Composite Structures* **2022,** 280, 114801. https://doi.org/10.1016/j.compstruct.2021.114801
[30] Shabeeb O., Mahjoob D., Mahan H. *et al.*: *IIUM Engineering Journal* **2022**, *23(2)*, 2182. https://doi.org/10.31436/iiumej.v23i2.2182
[31] Dalong H., Fangkun J., Dongbin O. *et al.*: *Progress in Organic Coatings* **2022**, *173*, 107158. https://doi.org/10.1016/j.porgcoat.2022.107158
[32] Komorek A., Szczepaniak R., Przybyłek P. *et al.*: *Composite Structures* **2021**, *256*, 113045. https://doi.org/10.1016/j.compstruct.2020.113045
[33] Xie W., Yang F., Meng S. *et al.*: *Composite Structures* **2020,** *245*, 112224. https://doi.org/10.1016/j.compstruct.2020.112224
[34] Rallini M., Puri I., Torre L. *et al.*: *Composite Structures* **2018**, *198*, 73. https://doi.org/10.1016/j.compstruct.2018.03.102
[35] Lombardi M., Fino P., Malucelli G. *et al.*: *Composite Structures* **2012,** *94(3)*, 1067. https://doi.org/10.1016/j.compstruct.2011.10.019
[36] Fino P., Lombardi M., Antonini A. *et al.*: *Composite Structures* **2012**, *94(3)*, 1060. https://doi.org/10.1016/j.compstruct.2011.10.020
[37] Szczepaniak R., Kozuń G., Przybyłek P. *et al.*: *Composite Structures* **2021**, *256*, 113041. https://doi.org/10.1016/j.compstruct.2020.113041
[38] Bakar M., Kucharczyk W., Stawarz S. *et al.*: *Composite Structures* **2021**, *259*, 113450. https://doi.org/10.1016/j.compstruct.2020.113450
[39] Alagar M., Kumar A., Mahesh K. *et al.*: *European Polymer Journal* **2000**, *36(11)*, 2449. https://doi.org/10.1016/S0014-3057(00)00038-0
[40] Kim M., Choe J., Lee D.G.: *Composite Structures* **2016**, *158*, 227. https://doi.org/10.1016/j.compstruct.2016.09.029
[41] Shi S., Wang Y., Yan L. *et al.*: *Composite Structures* **2020**, *251*, 112623. https://doi.org/10.1016/j.compstruct.2020.112623
[42] Bieniaś J., Jakubczak P.: *Composite Structures* **2017**, *172*, 147. https://doi.org/10.1016/j.compstruct.2017.03.075
[43] Li W., Zhang Z., Zhu M *et al.*: *Applied Thermal Engineering* **2022**, *209*, 118313. https://doi.org/10.1016/j.applthermaleng.2022.118313
[44] Ciech Sarzyna Co. (Since 2024 Qemetica) Informative papers of products [in Polish]. Nowa Sarzyna, **2021**. https://qemetica.com/
[45] Sigma-Aldrich Co. Informative papers of products, 2018. https://www.sigmaaldrich.com
[46] Montgomery D. C.: "Design and analysis of experiments", John Wiley and Sons, New York, Sydney 2009, p. 68.

Received 20 XI 2024.
Accepted 6 XII 2024.